ADDENDUM C:

DNP via Thermal Mixing: Beyond the High Temperature Approximation

This addendum concerns an extension to low spin temperature of the treatment of Provotorov's theory and its application to dynamic nuclear polarization (DNP) via fast thermal mixing—Sections 4.3.1 to 4.3.3, 5.3.2, 5.3.3 and 8.3.3 of Essentials of Dynamic Nuclear Polarization, Spindrift Publications, 2016—henceforward shortly denoted as *EofDNP*. The extension itself is presented in [1]. Here we consider numerical methods to solve two sets of equations derived in that paper. The first part of this addendum concerns Equations (73) and (74) yielding the stationary state of the electron spin system. The second part is devoted to Equations (66) and (67) providing the evolution of the nuclear spin polarization in the case of fast thermal mixing. FORTRAN codes implementing these numerical methods are given in two appendices.

C.1 Stationary State of the Electron Spin System

C.1.1 Stationary Generalized Provotorov Equations

The extension of Provotorov's theory presented in [1] applies for ESR spectra $g(\omega)$ that are inhomogeneously broadened by g-tensor anisotropy. As in *EofDNP* we normalize these spectra, so

$$\int_{\infty}^{\infty} \mathrm{d}\omega\, g(\omega) \;=\; 1, \tag{1}$$

define their centre of gravity ω_0, such that

$$\int_{-\infty}^{\infty} \mathrm{d}\omega\, (\omega-\omega_0) g(\omega) \;=\; 0 \tag{2}$$

and their second moment

$$D^2 \;=\; \int_{-\infty}^{\infty} \mathrm{d}\omega\, (\omega-\omega_0)^2 g(\omega). \tag{3}$$

As discussed in [1], fast spectral diffusion assures that the electron spin polarization as a function of frequency can always be written in the shape

$$P(\omega) \;=\; \tanh \tfrac{1}{2}\big(\omega_0\alpha + (\omega-\omega_0)\beta_{\mathrm{NZ}}\big) \tag{4}$$

proposed by Provotorov. Thus the electron spin system is described by two inverse spin temperatures α and β_{NZ}. These are traditionally called the inverse electron Zeeman temperature and the inverse electron non-Zeeman temperature, though at low spin temperature neither the electron Zeeman energy

$$U_{\mathrm{Z}} \;=\; \tfrac{1}{2}\hbar\omega_0 \int_{-\infty}^{\infty} \mathrm{d}\omega\, g(\omega) P(\omega) \tag{5}$$

is solely determined by α, nor the electron non-Zeeman energy

$$U_{\rm NZ} \;=\; \tfrac{1}{2}\hbar \int_{-\infty}^{\infty} {\rm d}\omega\; (\omega-\omega_0) g(\omega) P(\omega) \tag{6}$$

is solely a function of $\beta_{\rm NZ}$.

We consider the stationary state that is reached after applying a microwave field with a frequency $\omega_{\rm m}$ and an amplitude B_1 for a long time. According to [1], in this stationary state

$$\begin{aligned} F_1 \;&=\; \int_{-\infty}^{\infty} {\rm d}\omega\; g(\omega) P_S(\omega) \;-\; P_{\rm L} \;+\; 2W(\omega_{\rm m}) T_{1S} P_S(\omega_{\rm m}) \qquad\qquad &=\; 0\,, \\ F_2 \;&=\; \int_{-\infty}^{\infty} {\rm d}\omega\; (\omega-\omega_0) g(\omega) P_S(\omega) + 2W(\omega_{\rm m}) T_{1S} (\omega_{\rm m}-\omega_0) P_S(\omega_{\rm m}) \;&=\; 0\,. \end{aligned} \tag{7}$$

In these equations

$$P_{\rm L} \;=\; \tanh \tfrac{1}{2}\omega_0 \beta_{\rm L}, \qquad\qquad \beta_{\rm L} \;=\; \frac{\hbar}{k_{\rm B} T_{\rm L}} \tag{8}$$

is the average electron spin polarization when the electron spin system is in thermal equilibrium with the lattice. Here $T_{\rm L}$ and $\beta_{\rm L}$ are the lattice temperature and the inverse lattice temperature, while $\hbar$ and $k_{\rm B}$ are Planck's and Boltzmann's constants. Furthermore

$$W(\omega_{\rm m}) \;=\; \tfrac{1}{2}\pi \omega_{1S}^2 g(\omega_{\rm m}), \qquad\qquad \omega_{1S} \;=\; \gamma_S B_1 \tag{9}$$

is the rate at which the microwave field induces electron spin flips. Here we ignore the anisotropy of the g-tensor and set γ_S to be the average gyromagnetic ratio of the electron spins.

C.1.2 Numerical Methods

Numerical solutions of the set of equations (7) are found using a Newton-Raphson method for nonlinear systems of equations described in [2]. To solve a set of n nonlinear equations

$$F_i(x_1, \cdots, x_j, \cdots, x_n) \;=\; 0, \tag{10}$$

we insert trial solutions x_j^0 and expand up to first order:

$$\begin{aligned} &F_i(x_1^0 + \delta x_1, \cdots, x_j + \delta x_j, \cdots, x_n + \delta x_n) \\ &\qquad =\; F_i(x_1^0, \cdots, x_j^0, \cdots, x_n^0) \;+\; \sum_{j=1}^{n} \left(\frac{\partial F_i}{\partial x_j} \right)_{x_j = x_j^0} \delta x_j \;+\; \cdots \end{aligned} \tag{11}$$

Next we solve the set of equations

$$\left(\frac{\partial F_i}{\partial x_j} \right)_{x_j = x_j^0} \delta x_j \;=\; 0, \tag{12}$$

and set new trial solutions equal to $x_j^0 + \delta x_j$. This process is continued until

$$\sum_{i=1}^{n} \left| F_i(x_1, \cdots, x_j, \cdots, x_n) \right| \tag{13}$$

is less than a pre-determined threshold.

To implement this method we need the derivatives of the functions F_1 and F_2 defined in (7). We determine them analytically. We recall (4) showing that $P(\omega)$ is a tangent hyperbolic function, and note that

$$\frac{\partial}{\partial x}\tanh x \;=\; 1-\tanh^2 x. \tag{14}$$

We furthermore recall (2) and (1). As a result we find:

$$\frac{\partial F_1}{\partial \alpha} \;=\; \tfrac{1}{2}\omega_0\left[1\;-\int_{-\infty}^{\infty}\mathrm{d}\omega\; g(\omega)P_S^2(\omega)\;+\;2W(\omega_\mathrm{m})T_{1S}\big(1-P_S^2(\omega_\mathrm{m})\big)\right], \tag{15}$$

$$\frac{\partial F_1}{\partial \beta_\mathrm{NZ}} \;=\; \tfrac{1}{2}\left[-\int_{-\infty}^{\infty}\mathrm{d}\omega\;(\omega-\omega_0)g(\omega)P_S^2(\omega) + 2W(\omega_\mathrm{m})T_{1S}(\omega_\mathrm{m}-\omega_0)\big(1-P_S^2(\omega_\mathrm{m})\big)\right], \tag{16}$$

$$\frac{\partial F_2}{\partial \alpha} \;=\; \tfrac{1}{2}\omega_0\left[-\int_{-\infty}^{\infty}\mathrm{d}\omega\;(\omega-\omega_0)g(\omega)P_S^2(\omega) + 2W(\omega_\mathrm{m})T_{1\mathrm{NZ}}(\omega_\mathrm{m}-\omega_0)\big(1-P_S^2(\omega_\mathrm{m})\big)\right], \tag{17}$$

$$\frac{\partial F_2}{\partial \beta_\mathrm{NZ}} \;=\; \tfrac{1}{2}\left[D^2-\int_{-\infty}^{\infty}\mathrm{d}\omega\;(\omega-\omega_0)^2 g(\omega)P_S^2(\omega) + 2W(\omega_\mathrm{m})T_{1\mathrm{NZ}}(\omega_\mathrm{m}-\omega_0)^2\big(1-P_S^2(\omega_\mathrm{m})\big)\right], \tag{18}$$

in which D^2 is given by (3).

C.1.3 Example Results

Figure 1 presents numerical solutions of (7) for $\beta_\mathrm{NZ}/\beta_\mathrm{L}$ as a function of the microwave frequency ω_m The calculation is performed for TEMPO in an externally applied magnetic field $B_0 = 3.4$ T, at a temperature $T_\mathrm{L} = 1.5$ K, and for five different strength of the microwave power, such that $s_0 = W(\omega_0)T_{1S} = 0.01$, 0.1, 1, 10 and 100 at the centre of gravity ω_0 of the ESR spectrum. This spectrum was determined by first calculating the exact spectrum of just the electron spin and the ^{14}N spin using the components of the g-tensor and the hyperfine tensor provided in [3]. Next we included the hyperfine and super-hyperfine interaction with the remaining nuclear spins by convoluting this spectrum with a Gaussian with a width of 7.1 MHz—see Addendum B to *EofDNP*.

For comparison Figure 2 presents results that would have been obtained using the high temperature approximation. In this figure expression (5.81) from *EofDNP*,

$$\frac{\beta_\mathrm{NZ}}{\beta_\mathrm{L}} \;=\; -\,\frac{2s_\mathrm{m}\omega_0(\omega_\mathrm{m}-\omega_0)}{2s_\mathrm{m}\big[(\omega_\mathrm{m}-\omega_0)^2+D^2\big]+D^2}, \tag{19}$$

is used to calculate the curves. Here $s_\mathrm{m} = W(\omega_\mathrm{m})T_{1S}$. Especially at the edges of the ESR spectrum and at weaker microwave powers the general equations (7) predict a

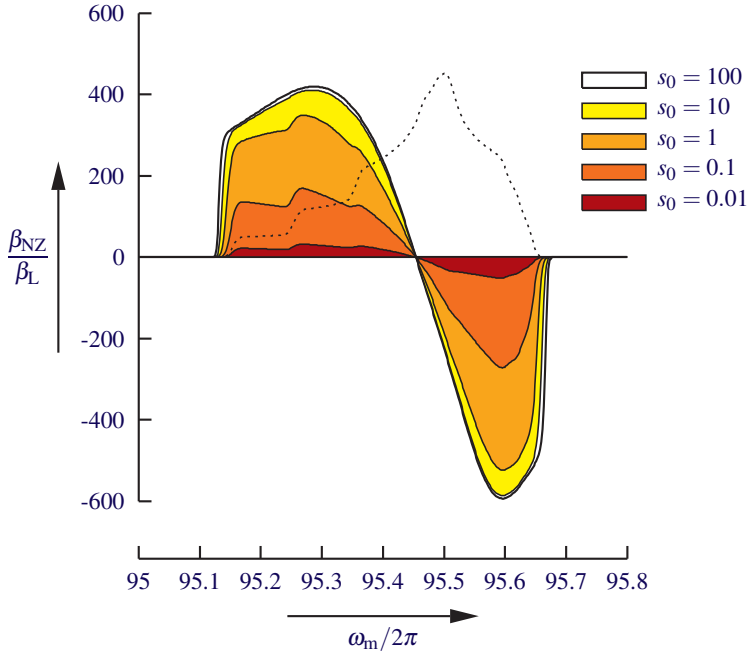

Figure 1: Example solutions of (7): β_{NZ}/β_L as a function of the microwave frequency ω_m for TEMPO in an externally applied magnetic field $B_0 = 3.4$ T, at a temperature $T_L = 1.5$ K and for five different strengths of the microwave power, such that $s_0 = W(\omega_0)T_{1S} = 0.01$, 0.1, 1, 10 and 100 at the centre of gravity of the ESR spectrum.

larger enhancement of the ratio β_{NZ}/β_L than the high temperature approximation. The reason is that the high temperature approximation does not take into account that the energy that can be stored in the electron non-Zeeman reservoir is considerably reduced when the electron spin polarization is high—see Section 4.3.1 of *EofDNP*. As a result the change of β_{NZ} is larger than predicted by the high temperature approximation.

C.2 Evolution of the Nuclear Spin Polarization

C.2.1 Equations for Fast Thermal Mixing

Figure 3 reproduces Figure 8.10 from *EofDNP* and shows the flows of energy in DNP via fast thermal mixing. Then the rate τ_{SSI}^{-1} of triple spin flips coupling the nuclear Zeeman reservoir to the electron non-Zeeman reservoir is much faster than all other processes. As a result the inverse nuclear Zeeman temperature β_I is always equal to the inverse electron non-Zeeman temperature β_{NZ}, and the polarization of nuclear spins $I = \frac{1}{2}$ is simple given by

$$P_I = \tanh \tfrac{1}{2}\omega_{0I}\beta_{NZ}, \tag{20}$$

in which ω_{0I} is the NMR frequency. Then the growth of the nuclear spin polarization

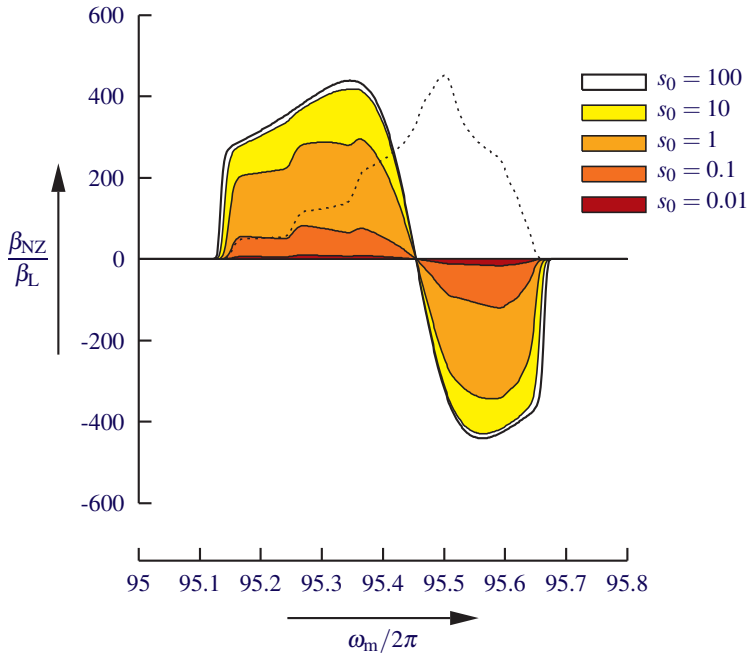

Figure 2: The high temperature approximation: expression (19) used to calculate β_{NZ}/β_L as a function of the microwave frequency ω_m for TEMPO in an externally applied magnetic field $B_0 = 3.4$ T and for five different strengths of the microwave power, such that $s_0 = W(\omega_0)T_{1S} = 0.01$, 0.1, 1, 10 and 100 at the centre of gravity of the ESR spectrum.

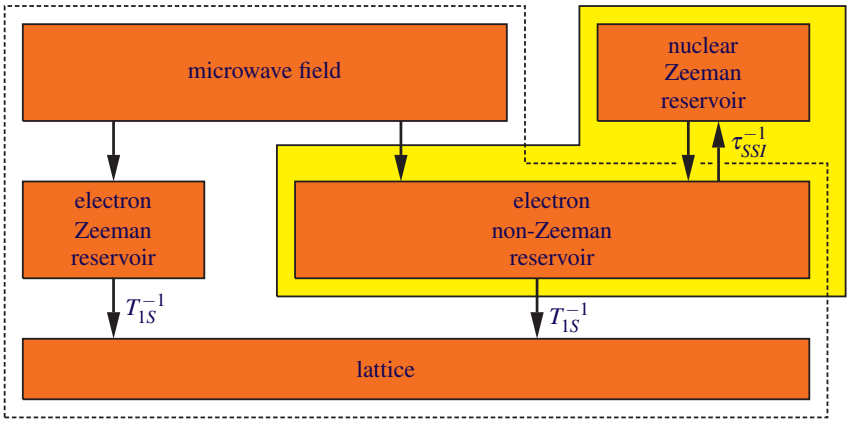

Figure 3: The flows of energy in DNP via fast thermal mixing.

as a function of time t can be solved from equations (66) and (67) in [1]:

$$\begin{aligned}
\omega_{0I}\frac{\partial P_I}{\partial t} &= -2W(\omega_{\rm m})\,\frac{N_S}{N_I}\,(\omega_{\rm m}-\omega_0)\tanh\tfrac{1}{2}\big(\omega_0\alpha+(\omega_{\rm m}-\omega_0)\beta_{\rm NZ}\big) \\
&\quad -\frac{1}{T_{1S}}\,\frac{N_S}{N_I}\int_{-\infty}^{\infty}\!\mathrm{d}\omega\; g(\omega)(\omega-\omega_0)\tanh\tfrac{1}{2}\big(\omega_0\alpha+(\omega-\omega_0)\beta_{\rm NZ}\big), \qquad (21) \\
0 &= -2W(\omega_{\rm m})\tanh\tfrac{1}{2}\big(\omega_0\alpha+(\omega_{\rm m}-\omega_0)\beta_{\rm NZ}\big) \\
&\quad -\frac{1}{T_{1S}}\left[\int_{-\infty}^{\infty}\!\mathrm{d}\omega\; g(\omega)\tanh\tfrac{1}{2}\big(\omega_0\alpha+(\omega-\omega_0)\beta_{\rm NZ}\big)\;-\;P_{\rm L}\right], \qquad (22)
\end{aligned}$$

in which N_S is the total number of electron spins, N_I is the total number of nuclear spins, while all other parameters are defined in Section C.1.1.

C.2.2 Numerical Methods and Example Solutions

The numerical code solves time t as a function of nuclear spin polarization P_I. First the inverse electron non-Zeeman temperature $\beta_{\rm NZ}$ as a function of P_I is solved from (20). Next, the inverse electron Zeeman temperature α as a function of $\beta_{\rm NZ}$ is determined using (22). Inserting the two inverse temperatures α and $\beta_{\rm NZ}$ in (21) then yields $\partial P_I/\partial t$ as a function of P_I. Finally, the integral

$$t \;=\; \int_0^{P_I}\mathrm{d}P_I'\,\left(\frac{\partial P_I'}{\partial t}\right)^{-1} \qquad (23)$$

yields time t as a function of the nuclear spin polarization P_I.

As an example Figure 4 shows the evolution of the proton spin polarization in a sample doped with TEMPO. The calculations were performed for $B_0 = 3.4$ T, $T_L = 1.5$ K, $\omega_{\rm m}/2\pi = 95.5828$ GHz and $s_0 = W_0T_{1S} = 100$, 10, 1, 0.1, where $W_0 = \pi\omega_{1S}^2 g(\omega_0)$. As in Figures 1 and 2 were determined using the method described in Addendum B of *EofDNP*. Notice that results for larger values of s_0 coincide with those for $s_0 = 100$.

References

[1] W.Th. Wenckebach: *J. Magn. Res.* (2017) DOI:10.1016/j.jmr.2017.01.020.

[2] W.H. Press, S.A. Teukolsky, W.T. Vetterling, B.P. Flannery: *Numerical Recipes in Fortran*, 2nd Ed., Cambridge University Press, Cambridge, 1992.

[3] S.T. Goertz, J. Harmsen, J. Heckmann, Ch. Hess, W. Meyer, E. Radtke, G. Reicherz: *Nucl. Instrum. Methods Phys. Res. A* 526 (2004) 43-52 DOI:10.1016/j.nima.2004.03.148.

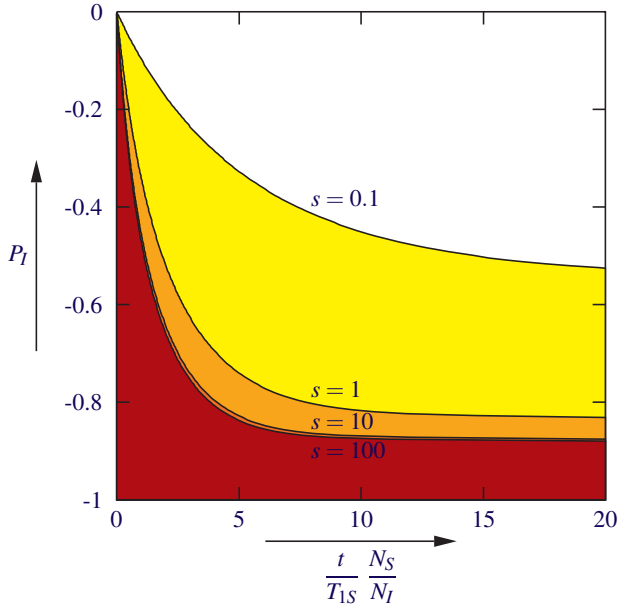

Figure 4: Evolution of the proton spin polarization for $B_0 = 3.4$ T, $T_L = 1.5$ K, $\omega_m/2\pi = 95.5828$ GHz and $s_0 = W_0 T_{1S} = 100$, 10, 1, 0.1, where $W_0 = \pi\omega_{1S}^2 g(\omega_0)$. Results for larger values of s_0 coincide with those for $s_0 = 100$.